

SUBSURFACE MAPPING OF FAULT STRUCTURE IN THE WEH ISLAND BY USING A 3D DENSITY OF GLOBAL GRAVITY

Faisal Abdullah*^{1,2}, Muhammad Yanis¹, Muhammad Haikal Razi^{1,3}, Muzakir Zainal¹, and Nazli Ismail^{1,2}

¹Department of Geophysical Engineering, Faculty of Engineering, Universitas Syiah Kuala, Indonesia

²Physics Department, Universitas Syiah Kuala, Darussalam-Banda Aceh 23111, Indonesia

³Geological Engineering Department, Gadjah Mada University, Yogyakarta 55281, Indonesia

*Corresponding Author, Received: 12 March 2022, Revised: 19 May 2022, Accepted: 12 June 2022

ABSTRACT: Indonesia's Aceh Province is an earthquake-prone area due to its location on the Great Sumatran Fault (GSF). Currently, earthquake mitigation by the local government constantly refers to the regional seismic hazard maps. However, some sources of an earthquake in the province which had caused damage to buildings and loss of human life were not easily traced to the fault on the surface. Currently, the mapping activities related to the Sumatra fault lines are only focused on the mainland. In contrast, the continuity of the GSF fault in the area of the sea and surrounding islands is very rarely studied. Weh Island is inhabited by many communities and has become a popular tourism area. This study aims to map the regional and local fault structure on the Weh Island using the gravity model plus (GGMPlus) data. We used the GGMPlus data with a resolution of 200 m for detailed mapping of regional and local faults. The 3D inversion of the GGMPlus data was carried out to obtain density parameters using two models, namely Singular Value Decomposition (SVD) and Occam optimization. The 3D inversion describes the presence of high-density rock blocks. A density value ranging between 2.72 - 2.96 gr/cm³ is interpreted as rocks with andesite-basaltic lava composition and lava or pyroclastic breccias resulting from local volcanic products as the rocks creating the island. Therefore, the zone interpreted as a local fault had a smaller density value (2.5 - 2.65 gr/cm³) than the surrounding.

Keywords: GGMPlus, Density structure, Fault, Weh Island.

1. INTRODUCTION

Apart from being located on the Indo-Australian Plate, Aceh Province is also traversed by the Sumatran Fault, which extends 1.900 km from the southern tip of Sumatra Island to the Andaman Sea. Along the fault line, there is a history of seismicity that occurred quite frequently, especially in the southern part of Sumatra. Meanwhile, its northern part has not shown a significant seismic activity since 170 years ago [1]. A previous study revealed that the Aceh region could experience earthquakes with a scale of $M_w \geq 7$ if the energy stored on the fault is not released due to the void of seismic activity. The earthquake is a severe threat to the Aceh region in the future. If the earthquake sources are on the mainland, the severity to the infrastructures and human life would be highly increased. The last three major earthquakes in the region (Takengon earthquake on 2 July 2013, Pidie Jaya earthquake on 6 July 2016 [2], and Tangse earthquake on 23 October 2013) with a magnitude of $SR < 6$ are examples of the serious threats. Figure 1 shows seismic activities in Aceh province obtained from USGS with a magnitude of $M_w > 3$ from 1980 to 2020.

Previous studies have been conducted to map the faults in several segments of Sumatra islands, such as one using geodetics [3], gravity [4], [5], and

seismology data and geological observations [1]. Therefore, the continuity of the faults to the ocean region and its surrounding islands is scarcely studied. However, Weh Island is an economic and strategic area in Aceh, and the local government has committed to developing the island for tourism [6]. In addition, Weh Island is located at the northwestern tip of Sumatra, which has been an earthquake void area for a long time [3]. In this study, we used GGMPlus data to map the fault structure in Weh Island. The GGMPlus data is high-resolution gravity data (230 m/px) developed from GRACE observation satellite with GOCE and added gravity ground data from databases around the world [7]. Compared to other gravity satellites, i.e., Topex, GOCE, and BGI free air, the GGMPlus

disturbance data has excellent accuracy and correlation with gravity ground data up to 95%. The satellite gravity data has been successfully employed for global investigations, including tectonic mechanism [5], [8], lithospheric and structure modeling [9], [10], basin area in oil field investigation [11], as well as the geological structure and fault mapping which combined with seismicity data [4]. Moreover, the gravity satellite data has been confirmed to possess an anomaly response equal to Shipborne Gravity data in the Indian Offshore Regions [12] and Hudson Bay [13].

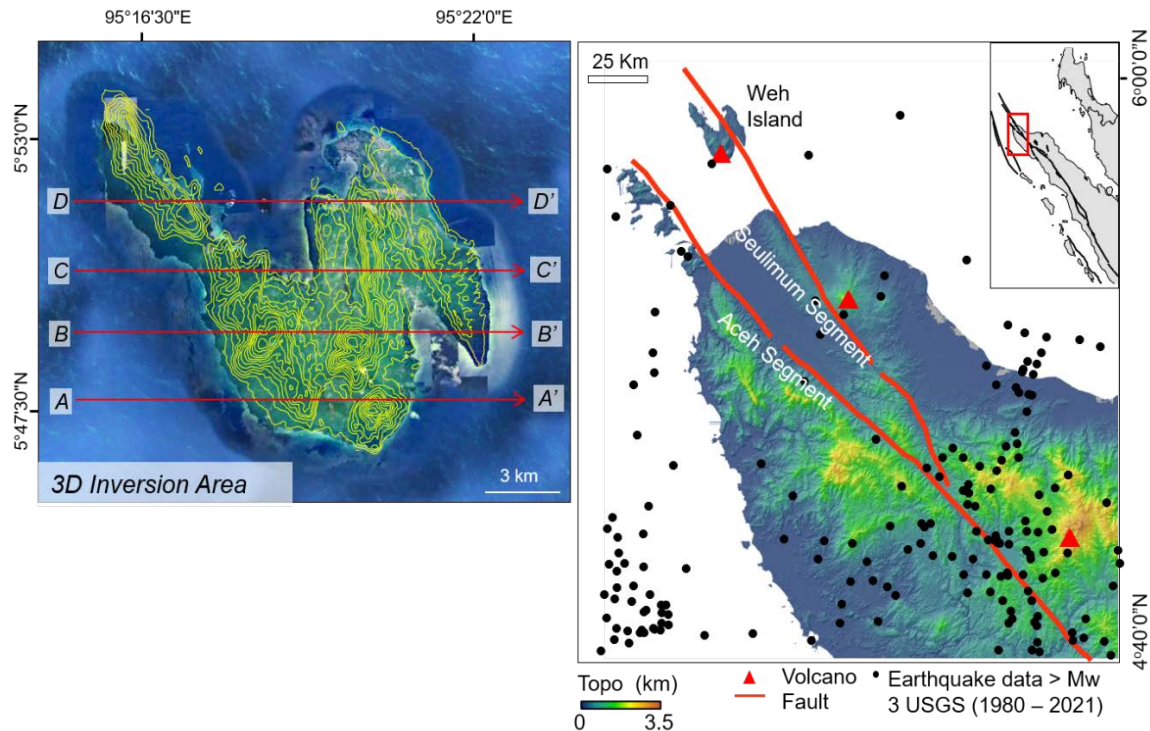


Fig. 1 Map of Sumatra Fault of Aceh and Seulimum Segmentation continuous to Weh Island overlaid with Mw > earthquake data from USGS (1980—2020) and the 3D inversion area map and 2D cross-section profile.

These facts allow the global gravity data to become the primary tool in investigating geological structures worldwide. Herein, we conducted 3D inversion of gravity data employing two models: Singular Value Decomposition (SVD) and Occam optimization.

2. RESEARCH SIGNIFICANCE

Gravity is one of the geophysical methods used to study the structure of the fault in the subsurface. The method is still conducted manually in the field; it will be constrained by the need for big finance and time-consuming on a large-scale area and a high topographic area such as in Indonesia, so the fault information is not yet available in all regions for disaster mitigation actions, especially on the small islands. This study applied the gravity model plus data with a high resolution of 200 m for detailed mapping of regional and local faults on the Weh Island. The gravity data were inverted using Singular Value Decomposition (SVD) and Occam algorithms to optimize the subsurface's density structure.

3. BACKGROUND AND GEOLOGICAL SETTINGS IN WEH ISLAND

The Weh Island is controlled by the active fault of the Great Sumatran Fault (GSF), which moves in a right-lateral direction to accommodate lateral mobility of Indo-Australia and Eurasia Plates

moving in oblique manner (7 mm/year) over the Sunda subduction system [1], [14]. Consequently, it impacts the high potential of seismic disaster and earthquake, acting as a primary factor against the ground motion in Sumatera Island during the last few decades. In a previous study, seismic activity of GSF could result in an earthquake up to $M=7.9$, along with other recorded earthquakes reaching $M=7.7$ along the Sumatera Fault [15]. Weh Island has a historical record of an earthquake with high intensity (up to $M=5.1$) distributed around the island with a depth of ± 10 km. A shallow earthquake location yielded more damage to the infrastructure on the surface. A detailed observation of Weh Island's morphology is mainly predominated by local fault structures possessing complex geological conditions, where out of 9 times of tectonic activities produce even fault structure. The fault structure in Weh Island is formed by tectonic movements along the GSF located on the northern part of the Sumatera Island [16]. In general, the fault structure formed in Weh Island is a normal fault, with horizontal slides located in the north-south and northwest-southeast directions [17].

Geomorphology of Weh Island has the high-hills topographical features on the southeast side with rock distribution of andesitic and basaltic, volcanoclastic, coral reefs, and alluvium [17]. The northwest-southeast and north-south sides have lower topography with rock distribution of tertiary sediments (Miocene), old volcanic rocks (quarter-

tertiary age) in forms of lava and pyroclastic flows, young volcanic rocks (quarter age) – products from the row of young volcanic cones forming a straight directed volcanic, as well as limestone reefs.

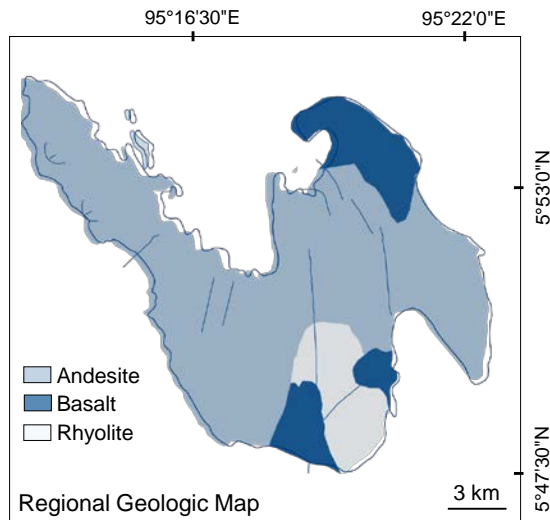


Fig. 2 Geological map of the Weh Island region showing the formation of rocks and the presence of geothermal manifestations.

4. METHODOLOGY

4.1 Basic Theory of GGMPlus

The basic principle of the gravity method lies in Newton's gravity law stating that gravity is proportional to the multiplication of two masses and inversely proportional to the quadratic distance between the two masses [18]. We used Global Gravity Model Plus data, a gravitational field model based on the topographical gravity, and data from satellites GOCE, EGM 2008, and Satellite GRACE. According to Rexer and Hirt [19], GGMplus could yield a complete description of the Earth's gravity at a very high resolution with a wide range. The GGMPlus data provide a parameter of gravity acceleration, radial, and horizontal field components, in a grid form with spaces between the points of ~ 220 m. On GGMPlus data, there are three process combinations, including synthesis of gravitational field from spherical harmonics, forward modeling, and normal gravity calculation on the ground to obtain the gravitational model with high resolution.

The GRACE/GOCE data results were combined with ground gravity data EGM2008 using a full normal equation. The EGM2008 SHCs are treated as a set of a priori known parameters introduced into a least-squares process. The GGMPlus data can be downloaded freely at Western Australian Centre for Geodesy, Curtin University. Then the data were extracted in *.asci

XYZ file, which was carried out with the source code on Matlab provided by Curtin University. This extraction process yielded several data: gravity accelerations, gravity disturbances, geoid undulations, and vertical components from sensor satellite altimetry. In this study, there were 12.500 grid data obtained representing the entire studied locations.

4.2 Data Processing

The satellite gravity data require Bouguer and terrain correction to obtain a complete Bouguer anomaly. Free-air anomaly obtained therein could provide a correlation between gravity accelerations and the topography of the studied area. Nonetheless, the free-air anomaly could not represent the complete geological information on the studied region. The anomaly requires several Bouguer and terrain corrections to observe the presence of targeted anomalies. Bouguer correction was carried out to correct the gravity value affected by the height by calculating the mass effect of the surrounding rocks in the observation site. Before performing Bouguer correction, assumptions should be firstly determined for the rocks in the studied region, which was 2.67 gr/cm³ based on the average density of continental crust.

The value of mass density of this rock assumption will be used to calculate the Bouguer correction related to the mass density of rocks in the studied area. A simple Bouguer anomaly map could be used to investigate the thickness of the subsurface based on the rock mass effect in the observation site, thus resulting in gravity values that are in line with subsurface mass density. But this gravity value is not yet accurate due to the field effect of the hilly observation sites and valley leading to Hammer's correction chart's employment, more known as terrain correction. This correction aimed to produce a gravitational value that is more accurate; by obtaining the value of the complete Bouguer anomaly. The gravity data obtained from satellite observation in the form of free air (Δg_{FA}) which is processed through Eq. 1;

$$\Delta g_{FA} = g_{Obs} + \delta g_{FA^S} + \delta g_{AC} - \gamma \quad \text{Eq. 1}$$

Where g_{Obs} is the observed gravity data, δg_{FA^S} is the second-order reduction of free air data, δg_{AC} is the atmospheric mass correction value and γ is the normal gravity parameter on the reference ellipsoid.

5. RESULT AND DISCUSSION

5.1 Bouguer Anomaly

A free-air correction was conducted to remove the effect of height in each measuring site. Free-air anomaly is the value of gravitational acceleration

affected by the topography. The gravity data obtained from the satellites are the free-air anomaly data which means that the data do not require a free-air correction anymore [19]. An obtained Free-air anomaly in this study, as shown in Fig.3, suggests a correlation between gravity accelerations and the topography of the investigated area. However, it could not present the entire geological information of the studied area. It requires several corrections further to observe the presence of an anomaly in this study.

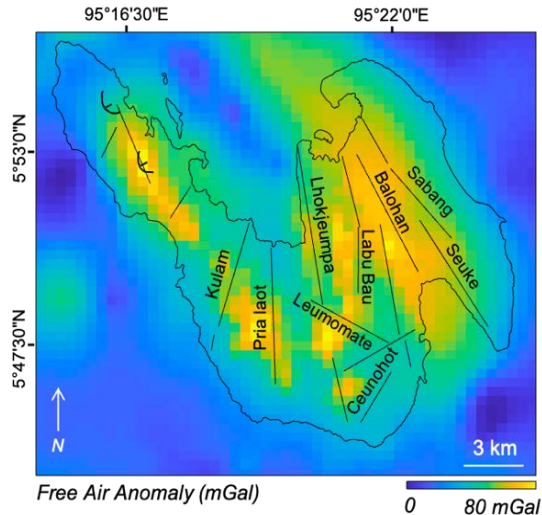


Fig.3 Free-air anomaly obtained from GGM+

Simple Bouguer anomaly data could investigate subsurface density based on the rock mass effect in the measuring site area, resulting in gravity values in line with the subsurface mass density. However, this gravity value is not yet accurate ascribed to the impact of the field of the studied area, hilly and valley. Therefore, a terrain correction should be performed to obtain the Bouguer anomaly's complete value to produce a more accurate gravity value.

The Bouguer anomaly, performed with terrain correction, would represent the subsurface gravity value that is only affected by the density of subsurface rocks. A complete Bouguer anomaly value was obtained after the terrain correction between 32 - 78 mGal, as shown in Fig.4. The region with low anomaly dominates the southern part of Weh Island with the anomaly value range of 32 - 50 mGal. The one dominating the island's central area has a range of anomaly values between 50 - 62 mGal. Meanwhile, the region with a high anomaly value had the range of 62 - 78 mGal dominating the eastern part of Weh Island. Lithologically, the studied area is consisted of rock formation with varied rock density, causing different gravity anomaly responses from one

location to another. In addition, there is a slide on the subsurface structure associated with the presence of the fault causing the difference in height from the structure, which further leads to the density contrast.

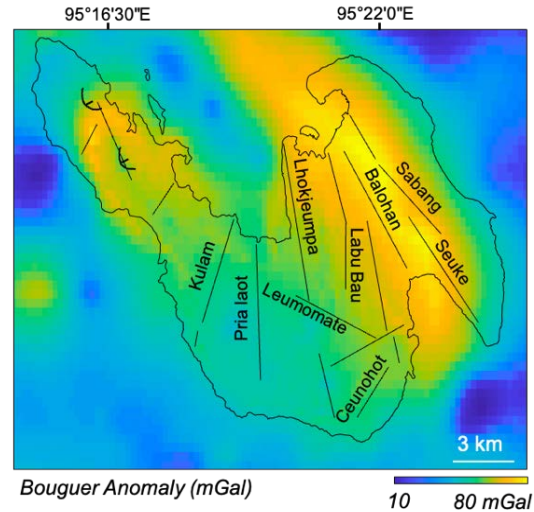


Fig.4 complete anomaly Bouguer with rock density assumption of 2.67 g/cm³.

5.2 3D Density Structure

The 3D modeling conducted herein aimed to observe the subsurface condition and its correlation with the presence of fault structure based on geological information from the investigation sites. The data optimization process was carried out using Grablox version 1.6 utilizing Singular Value Decomposition (SVD) and Occam optimization [20]. Both of the inversions were performed sequentially. If the optimization process with SVD results in a mismatch between the calculated density data with the measurement data, the Occam optimization would be carried out so that both types of data could be closely matched. The Occam is one of the inversion techniques that can be employed for electromagnetic data [21], [22]. The optimization process would allow error values between the observational and theoretical data to become smaller in their density or dimensions. The error value indicates the matching of the data. Thus, the model density resulting therein could be considered an optimum model.

The background density was 2.4, and the parameter of 2.67 was a response from volcanic rocks on the island. For the initial model, the X-axis was divided into 60 blocks (NX), Y-axis – 80 blocks (NY), and Z-axis – 30 blocks (NZ). Figure 5 shows a variation of density values in the area based on specific depths of 0 km and 7.5 km, while Figure 6 shows the density depth of 15 km and 22 km.

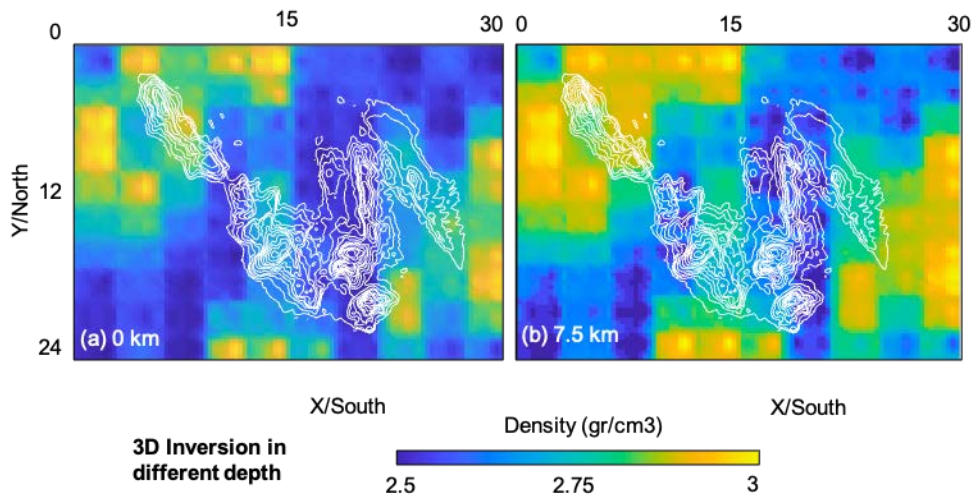


Fig. 5. The 3D model of gravity inversion with a depth of 0 and 7.5 km

The size of the studied region modeled herein was 30 km to the X-axis direction and 25 km to the Y-axis direction, while the targeted depth of the model (Z-axis) was 30 km. Due to its ambiguity, the depth in gravity modeling required information from other data. The solution depth given was 24 km obtained from the analysis of seismicity data from USGS from 1980 – to 2021. With a computer core i5 and RAM of 16 GB, it required ± 76 hours to complete the whole inversion, with five iterations to get the best solution model using SVD and Occam,

which reached the RMS errors up to 6.8%. Regions with relatively low density are dominated by alluvial, which consists of rearrangement of various types of old and young rocks with the size of laces up to caracal deposited on the ground, such as in estuary, coastal area, Seunara Swamp, Karing, Balohan Beach. Moreover, the coastal zone is dominated by limestone reefs stretched across the eastern beach resembling low hills up to the north, becoming the basis of Sabang City.

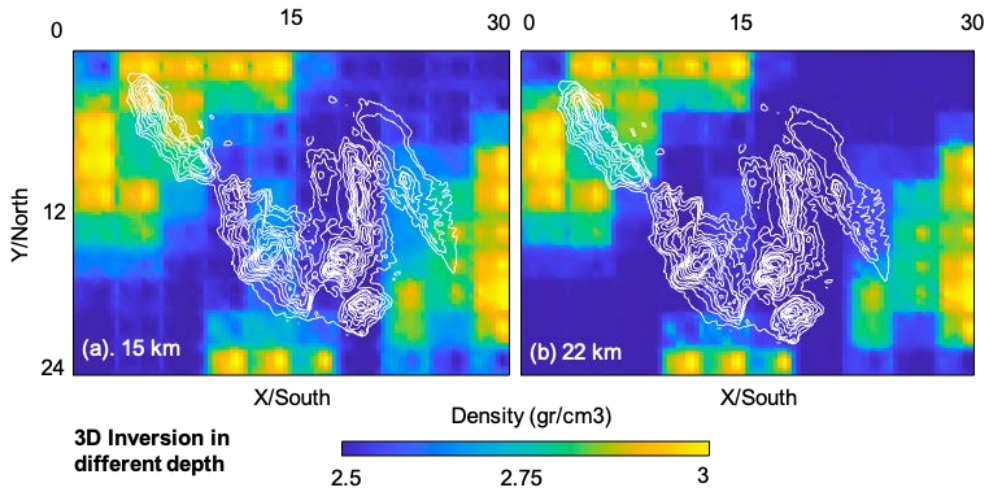


Fig. 6. The 3D model of gravity inversion with 15 and 22 km depth.

Meanwhile, layers at a depth of 12 km and 24 km have more variation in density, which is found within the range of $2.5 - 3 \text{ gr/cm}^3$, with an average density reaching 2.67 gr/cm^3 . It is estimated that these layers are dominated by a group of old volcanic rocks of Weh Island aged quarter-tertiary in the form of lava and pyroclastic flows. A group of young volcanic rocks aged quarter is the product of young volcanic rows forming directional volcanic straightness towards the northwest-

southeast and north-south. To interpret its specific locations, it is required to perform a cross-sectional analysis against the X and Y axis so that the density variations can be correlated with its local geological conditions. For this study, there are four cross-sections of the x-axis intersecting with its Y-axis. The results suggest the density values in the Weh Island region range between $2.5 - 3 \text{ gr/cm}^3$ with an overall average density of 2.6 gr/cm^3 . The obtained density model exhibits a general subsurface density

distribution in the studied area. The density values from each depth reveal a similar pattern, but the values tend to change as the depth increases. In general, layers of 0 km and 7.5 km had a close range of density variation (2.5 - 2.8 gr/cm³) with an average of 2.65 gr/cm³.

The four profiles are considered sufficient as a representative of the studied area. The trajectory of slices A-A' is 22 km from the measurement area, slices B-B' has 18 km shown in Fig.7, while the section of C-C' has 15 km, and D-D' has 10 km shown in Fig 8. These slices were selected based on the difference in density distribution on the cross-section obtained from the model and on the variation of the geological condition of the studied region. The difference in anomaly value received indicates the difference between the density of the rock layer in the studied location.

Results of this 2D interpretation show the density distribution laterally. Out of 4 cross-sections, the geological correlation was obtained because their locations are not too distant and are still within one similar geological structure. Rocks with high density were identified as volcanic zone correlated with the local geothermal system. As suspected, the rocks were initially magma and became immobile, forming igneous rocks. The volcano on the north-south side is a lava area with rock components of andesite-basaltic and pyroclastics. These volcanic rocks had a density of around 2.72 to 2.96 gr/cm³. These density values were affected by several things, which were rock composition and their formation. Intrusive igneous rock has higher values as opposed to lava rocks or pyroclastics. Igneous rocks with an alkaline composition also have a higher density value than acidic igneous rocks of the Kulam Tua aged quarter.

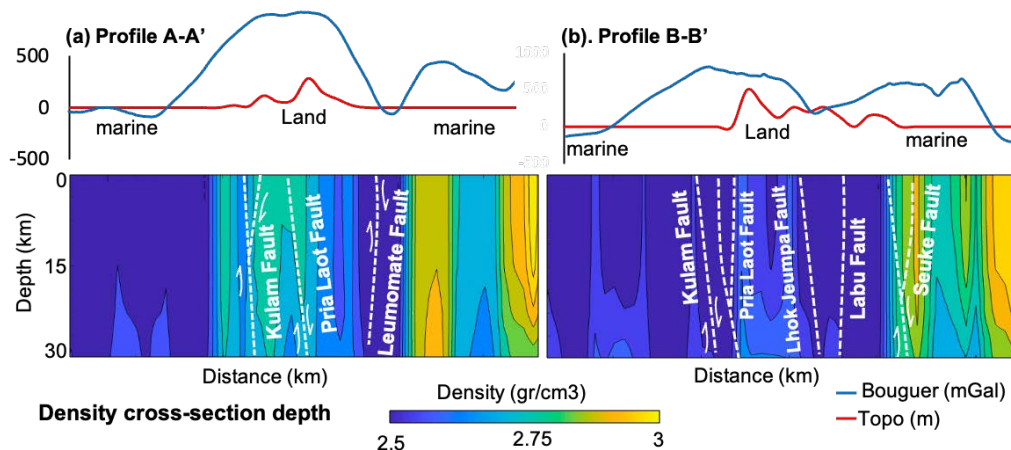


Fig.7 2D cross-section profile on A – A' and B-B' shows the density distribution against the depth. White lines represent local faults becoming the mechanism of the tectonic formation of Weh Island.

A cross-section model of 2D density on profile A-A' with a variation of density values on this location ranged between 2.50 and 2.82 gr/cm³. On profile A-A' (Fig.7a), an area indicated as a fault zone was located at a distance of 12 – 18 km from the 2D model. This region is interpreted as Kulam Fault, Pria Laot, and Leumo Matee fault structures. Kulam Fault structure is one of the normal faults with a north-south direction. The three faults are located with density values that are relatively lower (2.5 - 2.64 gr/cm³.) compared with the surrounding structure. The cross-section result shows a zone with density value reduction at a 20-km distance geologically in line with the intersection of the Leumo Matee fault. A part of the zone with moderate to high density dominates from 25 – 30 km, interpreted as the formation of pyroclastic flows of Leumo Matee. The density value increased significantly at 15-km up to 30-km depth, where the zone was still within one area of the volcanic site

Leumo Matee. Geologically, this region is dominated by pyroclastic flows centered in the volcano eruption.

The Density value at profile B-B'(Fig.7b) varied between 2.5 and 2.8 gr/cm³. A zone with moderate density (2.75 gr/cm³) was located at a distance of 15—30 km, interpreted as the formation of pyroclastic flows of Weh Island. Furthermore, several local faults aligned with the geological information [17]. The anomaly predicted with faults has a density contrast lower than the surrounding area; this is probably due to the subsidence of rock blocks. The five anomalies could be interpreted as the Kulam Fault, Pria Laot, Lhok Jeumpa, Labu Ba'U, and Seuke Fault. The fault zone had a low-density value ranging from 2.5 - 2.64 gr/cm³. There were no geothermal manifestations found at this location, but it was estimated that faults and fractures in this area were hydrological pathways from groundwater.

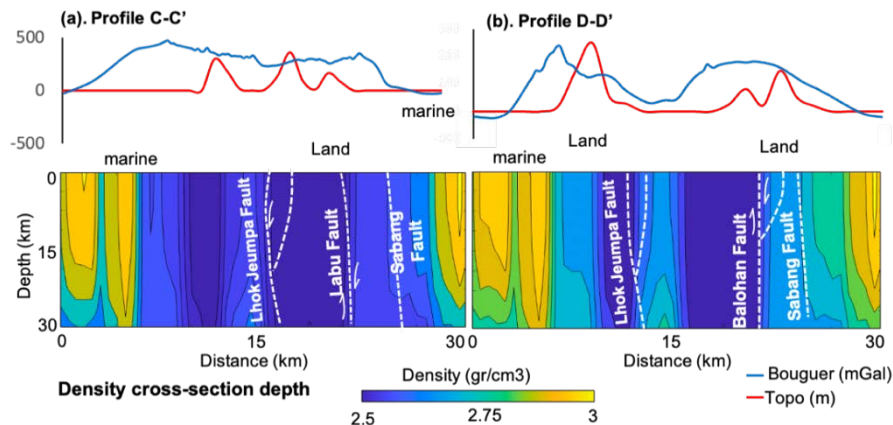


Fig.8. The 2D cross-section profile of C-C' and D – D' show density kontras correlated to fault area.

The area with a high density was located in the eastern part of the C-C section shown in Fig 8. a, interpreted as a volcanic rock structure in the forms of pyroclastic flows and lava of Weh Island. At profile D-D' in Fig. 8.b, the relatively high-density value was dominated at 0–8 km, interpreted as the Iboih Lava rock formation. This lava unit consists of lava and pyroclastic flows (tuff breccia) which went through in the lava and were andesitic-basaltic. The density value tends to increase as the depth increases at this location. A magmatic process was suspected to be associated with manifestations in the Iboih area [23]. Meanwhile, at a distance of 10–17 km, it had a low-density value ranging from 2.5 -2.57 gr/cm³, which was the location of Teluk Pria Laot that turned to the east from Pria Laot Bay. There were rocks with density values of 2.72 – 2.78 gr/cm³ to a depth of 20 km interpreted as Weh Lava rock groups. The results of the 2D cross-section, in general, have provided density contrast information that could describe several local faults, which are the main mechanisms creating Weh Island's tectonic activity.

6. CONCLUSIONS

The 3D modeling of GGMPlus data was carried out to delineate the local fault in Weh Island. In general. The resulted Bouguer anomaly ranged from 32 - 78 mGal, classified into low, moderate, and high anomaly areas. The low anomaly area was dominated in the southern part of the Weh Island, with anomaly values ranging from 32 to 50 mGal. The central zone is dominated by the anomaly values ranging from 50 to 62 mGal. Therefore, areas with high anomaly values, ranging from 62 to 78 mGal, dominated the eastern side of the Weh Island.

The results of 3D modeling show high rock density with values ranging from 2.72 to 2.96 gr/cm³ are interpreted as rocks with lava andesite-basaltic composition and lava or pyroclastic breccias produced by local volcanoes as the rocks creating the Weh Island. The zone indicated as a

fault had a smaller density value (2.5 - 2.65 gr/cm³) than the surrounding. The geological information showed a good correlation between the 2D cross-section model with the local fault location. The gravity satellite method can be considered very potential in determining subsurface geological structures in the Weh Island. Future research determining the correlation with geophysical methods is warranted.

7. ACKNOWLEDGMENT

This research is a part of the H-Index granted to Muhammad Yanis from Universitas Syiah Kuala by number 094/UN11.2.1/PT.01.03/PNBP/2022.

8. REFERENCES

- [1] Sieh K., and Natawidjaja D, Neotectonics of the Sumatran fault, Indonesia, *J. Geophys. Res. Solid Earth*, vol. 105, no. B12, pp. 28295–28326, Dec. 2000, doi: 10.1029/2000JB900120.
- [2] Marwan, Asrillah, Yanis. M., and Furumoto. Y., Lithological identification of devastated area by Pidie Jaya earthquake through Poisson's ratio analysis, *Int. J. GEOMATE*, vol. 17, no. 63, pp. 210–216, Nov. 2019, doi: 10.21660/2019.63.77489.
- [3] Ito. T., Gunawan. E., Kimata. F., Tabei. T., Simons. M., Meilano. I., Agustan, Otha. Y., Nurdin. I., and Sugiyanto, D., Isolating along-strike variations in the depth extent of shallow creep and fault locking on the northern Great Sumatran Fault, *J. Geophys. Res. Solid Earth*, vol. 117, no. B6, p. n/a-n/a, Jun. 2012, doi: 10.1029/2011JB008940.
- [4] Yanis. M., Faisal. A., Yenny. A., Muzakir. Z., Abubakar. M., and Nazli. I., Continuity of Great Sumatran Fault in the Marine Area revealed by 3D Inversion of Gravity Data, *J. Teknol.*, vol. 83, no. 1, pp. 145–155, Dec. 2020, 10.11113/jurnalteknologi.v83.14824.

- [5] Yanis. M., Abdullah. F., Zaini. N., and Ismail. N., The northernmost part of the Great Sumatran Fault map and images derived from gravity anomaly, *Acta Geophys.*, vol. 69, no. 3, pp. 795–807, Jun. 2021, doi: 10.1007/s11600-021-00567-9.
- [6] Marwan, Yanis. M., Muzakir, and Nugraha. G. S., Application of QR codes as a new communication technology and interactive tourist guide in Jaboi, Sabang, in *IOP Conference Series: Materials Science and Engineering*, Apr. 2020, vol. 796, no. 1, doi: 10.1088/1757-899X/796/1/012025.
- [7] Hirt. C., Kuhn. M., Claessens. S., Pail. R., Seitz. K., and Gruber. T., Study of the Earth's short-scale gravity field using the ERTM2160 gravity model, *Comput. Geosci.*, 2014.
- [8] Qu. W., Han. Y., Lu. Z., An. D., Zhang. Q., and Gao. Y., Co-seismic and post-seismic temporal and spatial gravity changes of the 2010 Mw 8.8 maule Chile earthquake Observed by GRACE and GRACE follow-on, *Remote Sens.*, vol. 12, no. 17, 2020, doi: 10.3390/RS12172768.
- [9] Radhakrishna. M., Lasith. S., and Mukhopadhyay. M., Seismicity, gravity anomalies and lithospheric structure of the Andaman arc, NE Indian Ocean, *Tectonophysics*, vol. 460, no. 1–4, pp. 248–262, Nov. 2008, doi: 10.1016/j.tecto.2008.08.021.
- [10] Bouman. J., Ebbing. J., Meekes. S., Fattah. R. A., Fuchs. M., Gradmann. S., Haagmans. R., Lieb. V., Schmidt. M., Dettmering. D., and Bosch. W., GOCE gravity gradient data for lithospheric modeling, *Int. J. Appl. Earth Obs. Geoinf.*, vol. 35, no. PA, pp. 16–30, 2015, doi: 10.1016/j.jag.2013.11.001.
- [11] Yanis. M., and Marwan, The potential use of satellite gravity data for oil prospecting in Tanimbar Basin, Eastern Indonesia, *IOP Conf. Ser. Earth Environ. Sci.*, vol. 364, no. 1, p. 012032, Dec. 2019, doi: 10.1088/1755-1315/364/1/012032.
- [12] Chatterjee. S., Bhattacharyya. R., Michael. L., Krishna. K. S., and Majumdar. T. J., Validation of ERS-1 and High-Resolution Satellite Gravity with in-situ Shipborne Gravity over the Indian Offshore Regions: Accuracies and Implications to Subsurface Modeling, *Mar. Geod.*, vol. 30, no. 3, pp. 197–216, Aug. 2007, doi: 10.1080/01490410701438323.
- [13] Keating. P., and Pinet. N., Comparison of surface and shipborne gravity data with satellite-altimeter gravity data in Hudson Bay, *Lead. Edge*, vol. 32, no. 4, pp. 450–458, 2013.
- [14] Rizal. M., Ismail. N., Yanis. M., Muzakir, and Surbakti. M. S., The 2D resistivity modeling on north sSumatranfault structure by using magnetotelluric data, *IOP Conf. Ser. Earth Environ. Sci.*, vol. 364, no. 1, p. 012036, Dec. 2019, doi: 10.1088/1755-1315/364/1/012036.
- [15] Petersen. M., Harmsen. S., Mueller. C., Haller. K., Dewey. J., Luco. N., Crone. A., Lidke. D., and Rukstales, K., Documentation for the Southeast Asia seismic hazard maps. Administrative Report September 2007, 30: 2007.
- [16] Yanis. M., Marwan. M., and Ismail. N., Efficient Use of Satellite Gravity Anomalies for mapping the Great Sumatran Fault in Aceh Province, Indones. *J. Appl. Phys.*, vol. 9, no. 02, p. 61, 2019, doi: 10.13057/ijap.v9i2.34479.
- [17] Dirasutisna. S., and Hasan. A., *Geologi Panas Bumi Jaboi, Sabang, Provinsi Aceh Nanggroe Darussalam*, pp. 1–6, 2005.
- [18] Ismail. N., Yanis. M., Abdullah. F., Irfansyam. A., and Atmojo. B. S. W., Mapping buried ancient structure using gravity method: A case study from Cot Sidi Abdullah, North Aceh, 2018, doi: 10.1088/1742-6596/1120/1/012035.
- [19] Rexer. M., and Hirt. C., Spectral analysis of the Earth's topographic potential via 2D-DFT: a new data-based degree variance model to degree 90,000, vol. 89, no. 9. 2015.
- [20] Pirttijarvi. M., Gravity interpretation and modeling software based on a 3-D block model, 2004.
- [21] Marwan, Yanis. M., Idroes. R., and Ismail. N., 2D inversion and static shift of MT and TEM data for imaging the geothermal resources of Seulawah Agam Volcano, Indonesia, *Int. J. GEOMATE*, vol. 17, no. 62, pp. 173–180, Oct. 2019, doi: 10.21660/2019.62.11724.
- [22] Marwan. M., Yanis. M., Nugraha. G. S., Zainal. M., Arahman. N., Idroes. R., Dharma. D. B., and Gunawan. P., Mapping of Fault and Hydrothermal System beneath the Seulawah Volcano Inferred from a Magnetotellurics Structure, *Energies*, vol. 14, no. 19, p. 6091, Sep. 2021, doi: 10.3390/en14196091.
- [23] Yanis. M., Ismail. N., and Abdullah. F., Shallow Structure Fault and Fracture Mapping in Jaboi Volcano, Indonesia, Using VLF–EM and Electrical Resistivity Methods, *Nat. Resour. Res.*, vol. 31, no. 1, pp. 335–352, Feb. 2022, doi: 10.1007/s11053-021-09966-7.